

# Modeling and Analysis of Smart Timoshenko Beams with Piezoelectric materials

M. Adnan Elshafei\*, M. R. Ajala\*, A. M. Riad\*\*

\* Department of Aeronautics, \*\* Department of Mechanical Engineering,  
Military Technical Collage, Cairo, Egypt.

**Abstract:** In the present work, a finite element model is proposed to describe the response of isotropic and orthotropic beams with piezoelectric actuators due to applied mechanical loads as well as electrical load. The assumed field displacements of the beams are represented by First-order Shear Deformation Theory (FSDT), the Timoshenko beam theory. The equation of motion of the smart beam system is derived using the principle of virtual displacements. In finite element formulation a cubic shape function is used to represent the axial displacement, the transverse displacement is represented by a quadratic shape function, while and the normal rotation and the electric potential is represented by a linear shape function at each node. The shear correction factor is used to improve the obtained results. A MATLAB code is developed to formulate the model and compute the natural frequency and the static deformation of the proposed structure system. The obtained results are compared to the available results of other investigators, good agreement is generally obtained.

**Keywords:** Finite element method, piezoelectric materials, Timoshenko beam theory, composite materials mechanics, and smart structure system.

## Nomenclature

Symbol	Definition
$A$	Beam cross section area
$A_{ij}$	Laminate extensional stiffness coefficients
$b$	Width of beam element
$B_{ij}$	Laminate coupling stiffness coefficients
$C_{ijkl}$	Elastic constants
$D_{ij}$	Laminate bending stiffness coefficients
$D_i$	Electric displacements
$E$	Young's modulus
$E_1$ and $E_2$	Young's modulus of the fiber longitudinal and transversal directions
$E_k$	Electric field ( $E_k = -\nabla \phi$ )
$e_{ijk}$	Piezoelectric constituents' constants
$f_a, f_t$	Axial and transversal forces
$h$	Height of beam element
$H$	Electric enthalpy
$K_{qq}$	Mechanical stiffness matrix
$K_{\varphi\varphi}$	Electric stiffness matrix

$K_{q\varphi}$	Coupled mechanical - electrical stiffness matrix
$L$	Length of beam element
$M$	Mass matrix of the beam
$\ddot{q}$	The second derivative of the nodal displacement
$Q_{ij}$	Components of the lamina stiffness matrix
$T$	Kinetic energy
$U$	Total strain energy of the structure system
$W$	Work done due to external loads
$\gamma_{xz}$	Transversal shear strain in x-z plane
$\epsilon_x, \epsilon_y, \epsilon_z$	Linear strains in the x-, y-, and z-directions
$\epsilon_{ij}^s$	Permittivity constants
$\xi_i, \zeta_i$	Axial and transversal displacements shape functions
$\rho$	Mass density of structure material
$\sigma$	Surface charge
$\phi$	Electric potential

## Abbreviations

HSDT	Higher-order shear deformation Theory
SSDT	Second-order shear deformation Theory
FSDT	First-order shear deformation Theory
CBT	Classical beam Theory

## I. INTRODUCTION

Several researchers are interested in solving the solid and smart beams structures using different theories. They are also interested in considering the shear effects on their results. For solid beam structures, Reference [1] presented the solution of the governing equations for the bending of cross-ply laminated beams using the state-space concept in conjunction with the Jordan canonical form. They used the classical, first-order, second-order, and third-order beam theories in their analysis. They determined the exact solutions for symmetric and asymmetric cross-ply laminated beams with arbitrary boundary conditions subjected to arbitrary loads. They also studied the effect of shear deformation, number of layers, and the orthotropic ratio on the static response of composite beams. They found that the effect of shear deformation caused large differences between the predicted deflections by the classical beam theory and the higher order beam theories, especially when the ratio of beam length to its height was low. They also deduced that

the symmetric cross-ply stacking sequence gave a smaller response than those of asymmetric ones. In case of asymmetric cross-ply arrangements, they noticed for the same beam thickness that the beam deflection decreased with increasing the number of beam layers and the orthotropic ratio, respectively. Reference [2] developed a finite element model based on a higher-order shear deformation theory with Poisson's effect, in-plane inertia and rotary inertia. They concluded that: (i) the shear deformations decrease the natural frequencies of the beam, which in turn, decrease by increasing the material anisotropy, (ii) the clamped-free boundary condition exhibits the lowest frequencies, (iii) the increase of fiber orientation angle decreases the natural frequency, and (iv) the natural frequencies increase with the increase of the number of beam layers. Reference [3] studied the free vibration characteristics of laminated composite beams using a general finite element model based on a first-order deformation theory. The model accounted for bi-axial bending as well as torsion. They also studied the effect of beam geometry and boundary conditions on natural frequencies. Their obtained results explained the effect of shear-deformation on vibration frequencies for various angle of ply laminates. Reference [4] studied the in-plane free vibration problem of symmetric cross-ply laminated beams based on the transfer matrix method. They considered the rotary inertia, the shear, and the extensional deformation effects on the Timoshenko's beam analysis which gave good results compared to that of other investigators for the natural frequencies associated with the first and higher modes. For smart beam structures, Reference [5] used tetrahedral piezoelectric elements for vibration analysis. They introduced the concept of "static condensation of the electric potential degrees of freedom", which presents the electric potential and loads written in terms of the mechanical properties of the structure. Their study was considered as a reference for electro-elastic finite element modeling of smart structures. Reference [6] studied theoretically and experimentally the induced strain actuation of an intelligent structure. The general procedures for solving the strain energy equations with Rayleigh-Ritz technique were presented. The use of Ritz approximate solutions led to understand the system design parameters and to model the smart structure systems. Substantial agreement between the measured and predicted deformations was found. Their obtained results demonstrated that the induced strain actuation was effective for controlling the structure deformation. Reference [7] investigated two separate theories. In the first approach, the transverse displacement component is assumed to be constant through the-thickness; in the second, the transverse displacement is allowed to vary for the inclusion of the inter laminar normal strains and the through-the thickness piezoelectric component. In approaches, the in-plane displacements and the

electrostatic potential is assumed to have arbitrary piecewise linear variations through the thickness of the laminate. The results also indicate the ranges of applicability and limitations of simplified mechanical models of sensory/active composites. Also their predicted natural frequency was in good agreement with that of as in [8]. Reference [9] presented the results of dispersion wave propagation curves for beams with surface-bonded piezoelectric patches. They used Euler and Timoshenko models of beam theory. They introduced dispersion curves for different thickness ratios between the piezoelectric layer and the host beam structure. These curves were obtained by assuming a half-cycle cosine potential distribution in the transverse direction of the piezoelectric material. In addition, the phase velocity for wave number was close to infinity, and the cutoff frequencies based on the Timoshenko beam model were also presented. They predicted that the phase velocity decreased as thicker piezoelectric materials were used. In addition, the cut off frequency was a function of the ratio between the shear and flexural rigidities of the beam. Reference [10] presented finite element model dealing with either extension or shear actuation mechanisms. The poling direction was taken parallel to the transversely applied electric field for their first mechanism, and in the axial direction for the second one. They concluded that the shear actuation mechanism is more efficient than the extension one for stiff structures and thick piezoelectric actuators. Reference [11] developed a theoretical formulation to model a composite smart structure. Their model was based on a high order displacement field coupled with a layer-wise linear electric potential. They used a finite element formulation with a two node Hermitian element and layer-wise nodes to derive the main equations of motion. They predicted the deflection and curvature of the beam due to the variation of actuator locations and orientations. They deduced the following: (i) the linearity between tip displacement and voltage of piezoelectric polyvinylidene bimorph beam may not necessarily apply on the other structural configurations, (ii) as the substrate stiffness decreases, the obtained actuation increases, (iii) the position of the active actuator near the fixed end of a cantilever has a great effect on beam curvature, (iv) the increase of the actuator numbers can increase the beam deflection and curvature, and (v) the rotation of the substrate 20 degrees around the z-axis results-in increasing the deflection and voltage compared to the un-rotated one, and the greatest effect could achieve by rotating the actuators placed in the middle of the beam. Reference [12] presented analytical solutions determining the length and position of strain-induced patch actuators that controlled the static beam deflections. Their solutions were derived using the exact relationships between the bending solutions of the adopted Timoshenko beam theory and the corresponding quantities of the Euler-Bernoulli beam theory. Examples

of point deflection control for shear deformable beams subjected to various loads were presented to validate the use of their derived solutions. They discussed the importance of contributing the transverse shear deformation effects on controlling the beam deflection. They predicted that the error resulting due to neglecting the effect of transverse shear deformation represented only a few percent; such a level of accuracy might not be acceptable in applications where very precise control was required, e.g. MEM structures. Similarly, for beams where the shear parameter was substantially large, it would be erroneous to ignore the significant effect of transverse shear deformation. Reference [13] developed an efficient analytical model for piezoelectric bimorph based on the improved First-order Shear Deformation Theory (FSDT). Their model combined the equivalent single-layer approach for mechanical displacements and a layer wise-type modeling of the electric potential. Shear correction factor  $k_s$  was introduced to modify both the shear stress and the electric displacement of each layer. Excellent agreement between the model predictions with  $k_s = 8/9$  and the exact solutions was obtained for the resonant frequencies. The results of their model and their numerical analyses revealed that: (i) piezoelectric bimorphs have similar behavior for series and parallel arrangements under the same loading, (ii) in dynamic analysis, accurate bending vibration frequencies can be obtained by the model even for thick beam (Aspect ratio=5), whereas the classical elastic thin beam theory or plate theory gives low accurate results; (iii) in FSDT model, further investigation is needed for determining the value of shear correction factor of piezoelectric laminates. References [14] develop a new two-dimensional coupled electro-mechanical model for a thick laminated beam with piezoelectric layer and subjected to mechanical and electric loading. The model combined the first order shear deformation theory for the relatively thick elastic core and linear piezoelectric theory for the piezoelectric lamina. Rayleigh-Ritz method was adopted to model the displacement and potential fields of the beam, and the governing equations were finally derived using the variational energy principle. Their predicted results showed that the electric potential developed across the piezoelectric layer was linear through the thickness and the deflection response of the beam was proportional to the applied voltage. Reference [15] proposed a simple finite element model to describe the behavior of advanced Euler's smart beams with piezoelectric actuators, made of isotropic and/or orthotropic materials, when subjected to axial and transverse loads in addition to electrical load. Both the cubic and Lagrange interpolation functions are used to formulate the finite element for the electro-elastic model. The obtained results were compared with the corresponding predictions of other investigators and found reasonable. Reference [16] formulated a model for

shape control of piezoelectric structure and proposed general procedure for determining the distributed actuation input required to satisfy a partially specified displacement field for a generic piezoelectric shell structure. They concluded that under certain conditions, a servo-constraint that defines a finite number algebraic relations on the motion of the material points of the structure can be satisfied in steady state by an equivalent number of independent actuators. Application examples shown, the servo-constraint was based on actuating defined motion of a number of material points. However, the constraint can involve any number of material points; it is just that the number of constraints must be limited to the number of independent actuators. Reference [17] presented finite element for shell structures with piezoelectric actuators and sensors based on conventional 8-node shell formulation and the classical displacement theory. The element has described the transverse kinematics in order to consistently retain the full 3D piezoelectric coupling. Also layer-wise description of the electric degrees of freedom permits to account for embedded piezoelectric layers. Numerical results validated their implementation. Reference [18] proposed a finite elements model for the coupling of piezoelectric plate elements based on different through-the-thickness expansions and variational principles through the Arlequin method. The model was formulated on the basis of a unified formulation. Higher order, layer-wise and mixed finite elements were obtained via unified formulation. Computational cost was reduced assuming refined models only in those zones of the structure where high accuracy is needed. Numerical results show that the Arlequin method in the context of unified formulation couples sub-domains having different piezoelectric finite elements effectively. Reference [19] investigated the electro dynamical response of the piezoelectric buckled beam operating as a kinetic-to-electrical energy converter. The buckling structure was used to implement a bistable magnetic free vibration energy harvester. The analytical model of the system was derived from the first-order composite plate theory. They presented theoretical and experimental studies to compare the output response of a linear versus nonlinear dynamical regime of such a piezoelectric clamped-clamped beam.

In the present work, a finite element model has been proposed to predict the behavior of advanced smart Timoshenko beams with piezoelectric materials, made of isotropic and/or orthotropic materials, when subjected to axial and transverse loads in addition to electrical load. The constant transverse shear stresses predicted by the used Timoshenko beam theory are always corrected by introducing the shear correction factor. The value of this factor is determined by equating the strain energy due to transverse shear stresses with the strain energy due to the true transverse stresses predicted by the three-dimensional elasticity theory [20]. The equation of

motion is derived based on the principle virtual displacements. A MATLAB code is constructed to predict the behavior of advanced beam structure due to different mechanical and electrical loads at different boundary conditions.

## II. THEORETICAL FORMULATION

The displacements field equations of the beam are assumed as [1]:

$$u(x, z) = u_o(x) - z \left[ c_o \frac{dw}{dx} + c_1 \phi(x) \right] + c_2 z^2 \psi(x) + c_3 (z/h)^3 \left[ \phi(x) + \frac{dw}{dx} \right] \quad (1)$$

$$v(x, z) = 0$$

$$w(x, z) = w_o(x)$$

where  $u$ ,  $v$ , and  $w$  are the displacements field equations along the  $x$ ,  $y$  and  $z$  coordinates, respectively,  $u_o$  and  $w_o$  denote the displacements of a point  $(x, y, 0)$  at the mid plane, and  $\phi(x)$  and  $\psi(x)$  are the rotation angles of the cross-section as shown in Figure 1.

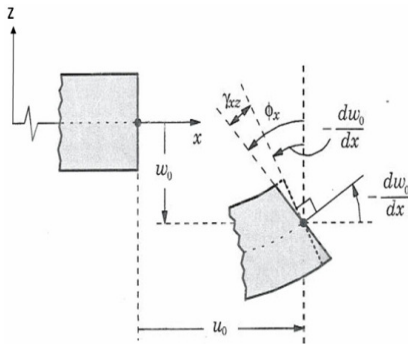


Fig 1. Deformed and un-deformed shape of Timoshenko beam [20].

Selecting the constant values of Eqn. (1) as:  $c_o = 0$ ,  $c_1 = 1$ ,  $c_2 = 0$ ,  $c_3 = 0$ , the displacements field equations for Timoshenko first-order shear deformation theory (FSDT) at any point through the thickness can be expressed as [20]:

$$\begin{aligned} u(x, z) &= u_o(x) - z\phi_x(x) \\ v(x, z) &= 0 \\ w(x, z) &= w_o(x) \end{aligned} \quad (2)$$

For one dimensional beam where the width in the  $y$ -direction is stress free and by using the plane stress assumption the remaining strain components are represented by differentiating the assumed displacement field equations, Eqn. (2), as follows:

$$\epsilon_{xx}(x, y, z) = \frac{\partial u(x, y, z)}{\partial x} = \frac{\partial u_o(x, z)}{\partial x} - z \frac{\partial \phi_x(x, z)}{\partial x} \quad (3a)$$

$$= \epsilon_{xx}^o + z\kappa_{xx}^o$$

$$\gamma_{xz}(x, y, z) = \frac{\partial u(x, y, z)}{\partial z} + \frac{\partial w(x, y, z)}{\partial x} \quad (3b)$$

$$= -\phi_x + \frac{dw_o}{dx} = \gamma_{xz}^o$$

The strains at any point through the thickness of the beam can be written in matrix form as:

$$\begin{Bmatrix} \epsilon_{xx} \\ \gamma_{xz} \end{Bmatrix} = \begin{Bmatrix} \epsilon_{xx}^o \\ \gamma_{xz}^o \end{Bmatrix} + z \begin{Bmatrix} \kappa_{xx}^o \\ \kappa_{xz}^o \end{Bmatrix} \quad (4a)$$

$$\begin{Bmatrix} \epsilon_{xx} \\ \gamma_{xz} \end{Bmatrix} = \begin{Bmatrix} \frac{\partial u_o}{\partial x} \\ -\phi_x + \frac{\partial w_o}{\partial x} \end{Bmatrix} + z \begin{Bmatrix} -\frac{\partial \phi_x}{\partial x} \\ 0 \end{Bmatrix} \quad (4b)$$

where  $\epsilon_{xx}^o$ ,  $\gamma_{xz}^o$  and  $\kappa_{xx}^o$  are the reference surface extensional strain in the  $x$ -direction, in-plane shear strain, and the curvature in the  $x$ -direction, respectively.

## III. PIEZOELECTRIC CONSTITUTIVE RELATIONS

In the linear piezoelectric theory, the electric enthalpy density  $H$  is expressed by [21]:

$$H = \frac{1}{2} c_{ijkl} \epsilon_{ij} \epsilon_{kl} - e_{kij} E_k \epsilon_{ij} - \frac{1}{2} \epsilon^s_{ij} E_i E_j \quad (5)$$

where  $c_{ijkl}$ ,  $e_{kij}$ , and  $\epsilon^s_{ij}$  are the elastic, piezoelectric, and permittivity constants, respectively. By taking the derivatives of Eqn.(5) with respect to the strain and the electric field components the piezoelectric constitutive equations can be obtained [22]-[23]:

$$\sigma_{ij} = c_{ijkl} \epsilon_{kl} - e_{ijk} E_k \quad (6)$$

$$D_i = e_{ikl} \epsilon_{kl} + \epsilon^s_{ik} E_k \quad (7)$$

where  $i, j = 1, \dots, 6$  and  $k, l = 1, \dots, 3$

The constitutive relations with plane stress approximation for  $k^{th}$  layer can be written as follows [24]:

$$\begin{Bmatrix} \sigma_1 \\ \sigma_2 \\ \sigma_3 \\ \sigma_6 \end{Bmatrix}_k = \begin{bmatrix} Q_{11} & Q_{12} & 0 & 0 & 0 \\ Q_{21} & Q_{22} & 0 & 0 & 0 \\ 0 & 0 & Q_{44} & 0 & 0 \\ 0 & 0 & 0 & Q_{55} & 0 \\ 0 & 0 & 0 & 0 & Q_{66} \end{bmatrix}_k \begin{Bmatrix} \epsilon_1 \\ \epsilon_2 \\ \epsilon_3 \\ \epsilon_6 \end{Bmatrix}_k - \begin{bmatrix} 0 & 0 & e'_{31} \\ 0 & 0 & e'_{32} \\ 0 & e'_{24} & 0 \\ e'_{15} & 0 & 0 \\ 0 & 0 & 0 \end{bmatrix}_k \begin{Bmatrix} E_1 \\ E_2 \\ E_3 \end{Bmatrix}_k \quad (8)$$

$$\begin{Bmatrix} D_1 \\ D_2 \\ D_3 \end{Bmatrix}_k = \begin{bmatrix} 0 & 0 & 0 & e'_{15} & 0 \\ 0 & 0 & e'_{24} & 0 & 0 \\ e'_{31} & e'_{32} & 0 & 0 & 0 \end{bmatrix}_k \begin{Bmatrix} \epsilon_{11} \\ \epsilon_{22} \\ \epsilon_{23} \\ \epsilon_{13} \\ \epsilon_{12} \end{Bmatrix}_k + \begin{bmatrix} \epsilon_{11}^s & 0 & 0 \\ 0 & \epsilon_{22}^s & 0 \\ 0 & 0 & \epsilon_{33}^s \end{bmatrix}_k \begin{Bmatrix} E_1 \\ E_2 \\ E_3 \end{Bmatrix}_k \quad (9)$$

where;

$$\begin{aligned} e'_{31} &= e_{31} - \frac{c_{13}}{c_{33}} e_{33}; & e'_{32} &= e_{32} - \frac{c_{23}}{c_{33}} e_{33}; \\ e'_{24} &= e_{24}; & e'_{15} &= e_{15}; \\ \epsilon_{11}^s &= \epsilon_{11}^s; & \epsilon_{22}^s &= \epsilon_{22}^s; & \epsilon_{33}^s &= \epsilon_{33}^s + \frac{e_{33}^2}{c_{33}} \end{aligned} \quad (10)$$

$c_{ij}^k$  are the elastic coefficients and  $Q_{ij}^k$  are the reduced stiffness coefficients related to the engineering constants for two cases as follows [25]:

**Case I: Isotropic layer**

$$\begin{aligned} Q_{11}^k &= Q_{22}^k = \frac{E}{1-\nu^2} & Q_{12}^k &= \frac{\nu E}{1-\nu^2} \\ Q_{44}^k &= Q_{55}^k = Q_{66}^k = G \end{aligned} \quad (11a)$$

where  $E$ ,  $G$ , and  $\nu$  are the isotropic material properties.

**Case II: Orthotropic layer**

$$\begin{aligned} Q_{11}^k &= \frac{E_1^k}{1-\nu_{12}^k \nu_{21}^k} & Q_{12}^k &= \frac{\nu_{12}^k E_2^k}{1-\nu_{12}^k \nu_{21}^k} \\ Q_{22}^k &= \frac{E_2^k}{1-\nu_{12}^k \nu_{21}^k} & Q_{44}^k &= G_{23} \\ Q_{55}^k &= G_{13} & Q_{66}^k &= G_{12} \end{aligned} \quad (11b)$$

Thus the transformed relation from the material principle axes 1, 2, and 3 to the geometrical axes x, y, and z can be written as:

$$\begin{Bmatrix} \sigma_{xx} \\ \sigma_{yy} \\ \sigma_{yz} \\ \sigma_{xz} \\ \sigma_{xy} \end{Bmatrix}_k = \begin{bmatrix} \bar{Q}_{11} & \bar{Q}_{12} & 0 & 0 & \bar{Q}_{16} \\ \bar{Q}_{21} & \bar{Q}_{22} & 0 & 0 & \bar{Q}_{26} \\ 0 & 0 & \bar{Q}_{44} & \bar{Q}_{45} & 0 \\ 0 & 0 & \bar{Q}_{45} & \bar{Q}_{55} & 0 \\ \bar{Q}_{16} & \bar{Q}_{26} & 0 & 0 & \bar{Q}_{66} \end{bmatrix}_k \begin{Bmatrix} \epsilon_{xx} \\ \epsilon_{yy} \\ \gamma_{yz} \\ \gamma_{xz} \\ \gamma_{xy} \end{Bmatrix}_k - \begin{bmatrix} 0 & 0 & \bar{e}_{31} \\ 0 & 0 & \bar{e}_{32} \\ \bar{e}_{14} & \bar{e}_{24} & 0 \\ \bar{e}_{15} & \bar{e}_{25} & 0 \\ 0 & 0 & \bar{e}_{36} \end{bmatrix}_k \begin{Bmatrix} E_x \\ E_y \\ E_z \end{Bmatrix}_k \quad (12)$$

$$\begin{Bmatrix} D_x \\ D_y \\ D_z \end{Bmatrix}_k = \begin{bmatrix} 0 & 0 & \bar{e}_{14} & \bar{e}_{15} & 0 \\ 0 & 0 & \bar{e}_{24} & \bar{e}_{25} & 0 \\ \bar{e}_{31} & \bar{e}_{32} & 0 & 0 & \bar{e}_{36} \end{bmatrix}_k \begin{Bmatrix} \epsilon_{xx} \\ \epsilon_{yy} \\ \gamma_{yz} \\ \gamma_{xz} \\ \gamma_{xy} \end{Bmatrix}_k + \begin{bmatrix} \bar{\epsilon}_{xx}^s & \bar{\epsilon}_{xy}^s & 0 \\ \bar{\epsilon}_{xy}^s & \bar{\epsilon}_{yy}^s & 0 \\ 0 & 0 & \bar{\epsilon}_{zz}^s \end{bmatrix}_k \begin{Bmatrix} E_x \\ E_y \\ E_z \end{Bmatrix}_k \quad (13)$$

where  $\bar{Q}_{ij}$  and  $\bar{e}_{ij}$  are the transformed reduced stiffness coefficients, and piezoelectric modules, respectively [25]. In the proposed model the following assumptions are used: (1) The width in y direction is stress free and the plane stress assumption is used. Therefore, it is possible to set  $\sigma_{yy} = \sigma_{yz} = \sigma_{xy} = \gamma_{yz} = \gamma_{xy} = 0$ , and  $\epsilon_{yy} \neq 0$ . (2) The polarization axis z is aligned with the thickness direction of the beam, thus only  $D_z$  in Eqn.(13) is taken into consideration. (3) By introducing  $E_z$  applied across the actuator thickness and the other components of the electric fields are zeros. (4) The coefficient  $e_{15}$  and  $\epsilon_{11}^s$  are neglected. Therefore the constitutive relations Eqn. (12) and Eqn. (13) are reduced to:

$$\begin{Bmatrix} \sigma_{xx} \\ \sigma_{xz} \\ D_z \end{Bmatrix}_k = \begin{bmatrix} \bar{Q}_{11} & 0 & 0 \\ 0 & k_s \bar{Q}_{55} & 0 \\ \bar{e}_{31} & 0 & 0 \end{bmatrix}_k \begin{Bmatrix} \epsilon_{xx} \\ \gamma_{xz} \\ 0 \end{Bmatrix}_k - \begin{bmatrix} \bar{e}_{31} \\ 0 \\ -\bar{\epsilon}_{zz}^s \end{bmatrix}_k E_z \quad (14)$$

where  $k_s$  is the shear correction factor and the other coefficients in Eqn. (14) are given by:

**Case I: Isotropic layer**

$$\bar{Q}_{11} = E \quad \bar{Q}_{55} = G, \text{ and } \bar{Q}_{ij} = Q_{ij} \quad (15a)$$

**Case II: Orthotropic layer**

$$\bar{Q}_{11} = \bar{Q}_{11} - \frac{\bar{Q}_{12} \bar{Q}_{12}}{\bar{Q}_{22}} \quad \bar{Q}_{55} = \bar{Q}_{55} - \frac{\bar{e}_{25} \bar{Q}_{45}}{\bar{e}_{24}} \quad (15b)$$

And the piezoelectric coefficients are given by:

$$\begin{aligned} \bar{\epsilon}_{zz}^s &= \bar{\epsilon}_{zz}^s + \frac{\bar{e}_{32} \bar{e}_{32}}{\bar{Q}_{22}} \\ \bar{e}_{31} &= \bar{e}_{31} - \bar{e}_{32} \frac{\bar{Q}_{12}}{\bar{Q}_{22}} & \bar{e}_{15} &= \bar{e}_{15} - \frac{\bar{e}_{25} \bar{e}_{14}}{\bar{e}_{24}} \end{aligned} \quad (16)$$

The electric field components are related to the electrostatic potential  $\phi$  by the equation [22]:

$$E_k = -\phi_{,k} \quad (17)$$

**IV. ENERGY FORMULATION**

The kinetic energy of the beam structure is given by [3]:

$$T = \frac{1}{2} \int_v \rho [\dot{u}^2 + \dot{w}^2] dv \quad (18)$$

The work done due to external mechanical and electrical loads is represented by [26]:

$$W = \int_0^L f_a u dx + \int_0^L f_t w dx + P_i w_i - \int_{S_1} \sigma \phi dS_1 \quad (19)$$

where  $f_a$ , and  $f_t$  are the transversal and axial forces along a surface with length  $L$ , respectively.  $P_i$ , is the concentrated force at point  $i$  and  $w_i$  is the corresponding generalized displacement,  $\sigma$  ( $C/m^2$ ) is the surface charge density on the actuator surface, and  $\phi$  is the electric potential at the piezoelectric surface area  $S_1$  at ( $z = h_p$ ).

The total internal strain energy for the structure system  $U$  is the sum of internal strain energy  $\hat{U}$ , and the electric field potential energy  $U_e$  such as [15]:

$$U = \frac{1}{2} \int_v (\hat{U} + U_e) dv \quad (20)$$

where

$$\hat{U} = \frac{1}{2} \int_v \epsilon_{kl} \sigma_{ij} dv \quad (21a)$$

$$U_e = \frac{1}{2} \int_v E_k D_i dv \quad (21b)$$

Thus total strain energy for the structure system  $U$  is expressed as:

$$U = \int_v \left[ \frac{1}{2} c_{ijkl} \epsilon_{ij} \epsilon_{kl} - e_{kij} E_k \epsilon_{ij} - \frac{1}{2} \epsilon_{ij}^s E_i E_j \right] dv \quad (22)$$

For the proposed beams it is given by:

$$U = \frac{1}{2} \int_v \left[ (\sigma_{xx} \epsilon_{xx} + k_s \sigma_{xz} \gamma_{xz}) - (D_z E_z) \right] dv \quad (23)$$

**Case I: Isotropic Beam:**

$$U = \frac{1}{2} \int_v \left[ E \epsilon_{xx}^2 + k_s G \gamma_{xz}^2 - 2\tilde{e}_{31} E_z \epsilon_{xx} - \tilde{e}_{zz}^s E_z^2 \right] dv \quad (24)$$

**Case II: Orthotropic Beam:**

$$U = \frac{1}{2} \int_v \left[ (\tilde{Q}_{11} \epsilon_{xx}^2 + k_s \tilde{Q}_{55} \gamma_{xz}^2 - 2\tilde{e}_{31} E_z \epsilon_{xx} - \tilde{e}_{zz}^s E_z^2) \right] dv \quad (25)$$

By substituting the strains components of Eqn. (2) in Eqns. (18), (19), (24), and (25) one can obtain the kinetic energy, the external work, and the strain energy for both beams equations.

$$T = \frac{1}{2} \int_v \left[ (\dot{u}_o - z \dot{\phi}_x)^2 + (\dot{w}_o)^2 \right] dv \quad (26)$$

$$W = \int_0^L f_a (u_o - z \phi_x) dx + \int_0^L f_t w_o dx + P_i w_{o_i} - \int_{S_1} \sigma \phi dS_1 \quad (27)$$

**Case I: Isotropic Beam:**

$$U = \int_v \left[ \frac{1}{2} \left[ E \left( \frac{\partial u_o}{\partial x} - z \frac{\partial \phi_x}{\partial x} \right)^2 + k_s G \left( -\phi_x + \frac{\partial w_o}{\partial x} \right)^2 \right] - \left[ \tilde{e}_{31} \left( -\frac{\partial \phi}{\partial z} \right) \left[ \left( \frac{\partial u_o}{\partial x} - z \frac{\partial \phi_x}{\partial x} \right) \right] - \frac{1}{2} \left( -\frac{\partial \phi}{\partial z} \right)^2 \tilde{\epsilon}_{zz}^s \right] \right] dv \quad (28a)$$

**Case II: Orthotropic Beam**

$$U = \int_v \left[ \frac{1}{2} \left[ \tilde{Q}_{11} \left( \frac{\partial u_o}{\partial x} - z \frac{\partial \phi_x}{\partial x} \right)^2 + k_s \tilde{Q}_{55} \left( -\phi_x + \frac{\partial w_o}{\partial x} \right)^2 \right] - \left[ \tilde{e}_{31} \left( -\frac{\partial \phi}{\partial z} \right) \left[ \left( \frac{\partial u_o}{\partial x} - z \frac{\partial \phi_x}{\partial x} \right) \right] - \frac{1}{2} \left( -\frac{\partial \phi}{\partial z} \right)^2 \tilde{\epsilon}_{zz}^s \right] \right] dv \quad (28b)$$

**V. FINITE ELEMENT FORMULATION**

A five nodes beam element with eleven degrees of freedom is shown in Figure 2. The element has nine mechanical degrees of freedom  $\{u, w, \phi_x\}$  which represent the axial, transverse, and rotational at the nodes, respectively and two electric degrees of freedom  $\{\phi\}$  [26]:

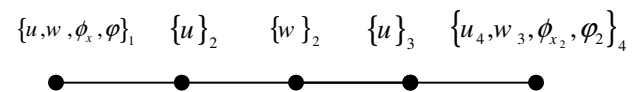


**Fig 2: Element nodal degrees of freedom.**

The axial displacement can be expressed in the nodal displacements as follows:

$$u(x) = u_1 \xi_1 + u_2 \xi_2 + u_3 \xi_3 + u_4 \xi_4 = \sum_{j=1}^4 u_j \xi_j \quad (29)$$

where the cubic shape functions  $\xi_j$  are found to be:

$$\begin{aligned} \xi_1 &= -\frac{9}{2} \left( \frac{x}{L} \right)^3 + 9 \left( \frac{x}{L} \right)^2 - \frac{11}{2} \left( \frac{x}{L} \right) + 1 \\ \xi_2 &= \frac{27}{2} \left( \frac{x}{L} \right)^3 - \frac{45}{2} \left( \frac{x}{L} \right)^2 + 9 \left( \frac{x}{L} \right) \\ \xi_3 &= \frac{-27}{2} \left( \frac{x}{L} \right)^3 + 18 \left( \frac{x}{L} \right)^2 - \frac{9}{2} \left( \frac{x}{L} \right) \\ \xi_4 &= \frac{9}{2} \left( \frac{x}{L} \right)^3 - \frac{9}{2} \left( \frac{x}{L} \right)^2 + \frac{x}{L} \end{aligned} \quad (30)$$

The transversal displacement  $w$  can be expressed in terms of nodal displacements as:

$$w(x) = w_1 \zeta_1 + w_2 \zeta_2 + w_3 \zeta_3 = \sum_{j=1}^3 w_j \zeta_j \quad (31)$$

where, the quadratic interpolation shape functions are given by:

$$\begin{aligned} \zeta_1 &= 1 - 3\left(\frac{x}{L}\right) + 2\left(\frac{x}{L}\right)^2 \\ \zeta_2 &= 4\left(\frac{x}{L}\right) - 4\left(\frac{x}{L}\right)^2 \\ \zeta_3 &= -\left(\frac{x}{L}\right) + 2\left(\frac{x}{L}\right)^2 \end{aligned} \quad (32)$$

The rotation angle  $\phi_x$  is expressed as:

$$\phi_x = \phi_1 \psi_1 + \phi_2 \psi_2 = \sum_{j=1}^2 \phi_j \psi_j \quad (33)$$

where the Linear interpolation shape functions  $\psi_j$  have the form:

$$\psi_j = 1 - \frac{x}{L}, \text{ and } \psi_j = \frac{x}{L} \quad (34)$$

In the proposed model the electric potential is considered as function of the thickness and the length of the beam [15]. In case of the electric potential is function of the length, it can be represented by:

$$\phi(x) = \phi_1 \hat{\zeta}_1 + \phi_2 \hat{\zeta}_2 = \sum_{j=1}^2 \phi_j \hat{\zeta}_j \quad (35)$$

where;

$$\hat{\zeta}_1 = 1 - \frac{x}{L}, \text{ and } \hat{\zeta}_2 = \frac{x}{L} \quad (36)$$

And in case the electric potential is function of the thickness of the beam, it can be given as:

$$\phi(z) = \phi_1 \check{\zeta}_1 + \phi_2 \check{\zeta}_2 = \sum_{j=1}^2 \phi_j \check{\zeta}_j \quad (37)$$

where;

$$\check{\zeta}_1 = \frac{1}{2} + \frac{z}{h}, \quad \check{\zeta}_2 = \frac{1}{2} - \frac{z}{h} \quad (38)$$

Thus by the product of equations (36) and (38) and impose the homogenous boundary condition on the bottom surface to eliminate the rigid body modes. Thus the electric potential can be written as:

$$\phi(x, 0, z) = \phi_1 \zeta_1 + \phi_2 \zeta_2 = \sum_{j=1}^2 \phi_j \zeta_j \quad (39)$$

And the shape functions are finally takes the form:

$$\zeta_1 = \left(\frac{1}{2} + \frac{z}{h}\right) \left(1 - \frac{x}{L}\right); \quad \zeta_2 = \left(\frac{1}{2} + \frac{z}{h}\right) \left(\frac{x}{L}\right) \quad (40)$$

## VI. VARIATION FORMULATION

By applying the principle of the virtual displacements to representative physical element of the beam such as:

$$\delta U = \delta W + \delta T \quad (41)$$

The first variation of the kinetic energy Eqn. (26) is expressed as:

$$\delta T = \int_V \rho \left[ \delta u_o^T (u_o - z \dot{\phi}_x) + \delta \dot{\phi}_x^T (-z u_o + z^2 \dot{\phi}_x) + \delta w_o^T w_o \right] dv \quad (42)$$

From equation (42) the elements of the mass matrix are given by:

$$\begin{aligned} M_{11} &= \int_{-b/2}^{b/2} \int_0^L (\delta u_o^T I_o u_o) dx dy \\ M_{12} &= M_{21} = 0 \\ M_{13} &= - \int_{-b/2}^{b/2} \int_0^L (\delta u_o I_{1\phi_x}) dx dy \\ M_{22} &= \int_{-b/2}^{b/2} \int_0^L (\delta w_o^T I_o w_o) dx dy \\ M_{23} &= M_{32} = 0 \\ M_{31} &= - \int_{-b/2}^{b/2} \int_0^L (\delta \dot{\phi}_x^T I_{1u_o}) dx dy \\ M_{33} &= \int_{-b/2}^{b/2} \int_0^L (\delta \dot{\phi}_x^T I_{2\phi_x}) dx dy \end{aligned} \quad (43)$$

and

$$(I_0, I_1, I_2) = \rho \int_{-h/2}^{h/2} (1, z, z^2) dz$$

where,  $I$  and  $\rho$  is the moment of inertia and the mass density of the material, respectively.

The first variation of the external work equation (27) takes the form:

$$\delta W = \int_0^L f_a (\delta u_o - z \delta \phi_x) dx + \int_0^L f_t \delta w_o dx + P_i \delta w_o - \int_{S_1} \sigma \delta \phi dS_1 \quad (44)$$

The first variation of the strain energy equation number (28)a takes the form:

**Case I: Isotropic Beam**

$$\delta U = \int_V \left[ E \left[ \left( \frac{\partial u_o}{\partial x} \delta \frac{\partial u_o}{\partial x} \right) - z \left( \frac{\partial u_o}{\partial x} \delta \frac{\partial \phi_x}{\partial x} + \frac{\partial \phi_x}{\partial x} \delta \frac{\partial u_o}{\partial x} \right) + z^2 \left( \frac{\partial \phi_x}{\partial x} \delta \frac{\partial \phi_x}{\partial x} \right) \right] + k_s G \left[ \left( \phi_x \delta \phi_x \right) - \left( \phi_x \delta \frac{\partial w_o}{\partial x} + \frac{\partial w_o}{\partial x} \delta \phi_x \right) + \left( \frac{\partial w_o}{\partial x} \delta \frac{\partial w_o}{\partial x} \right) \right] + \tilde{e}_{31} \left[ \left( \frac{\partial u_o}{\partial x} \delta \frac{\partial \phi}{\partial z} + \frac{\partial \phi}{\partial z} \delta \frac{\partial u_o}{\partial x} \right) - z \left( \frac{\partial \phi_x}{\partial x} \delta \frac{\partial \phi}{\partial z} + \frac{\partial \phi}{\partial z} \delta \frac{\partial \phi_x}{\partial x} \right) \right] - \tilde{e}_{ss} \left[ \left( \frac{\partial \phi}{\partial z} \delta \frac{\partial \phi}{\partial z} \right) \right] \right] dv \quad (45)$$

Thus the elements of the stiffness matrix of isotropic beam can be written as:

$$\begin{aligned} k_{11} &= E \int_{-b/2}^{b/2} \int_0^L \left( \frac{\partial u_o^T}{\partial x} \delta \frac{\partial u_o}{\delta x} \right) dx dy \\ k_{12} &= 0 \\ k_{13} &= -Ez \int_{-b/2}^{b/2} \int_0^L \left( \frac{\partial u_o^T}{\partial x} \delta \frac{\partial \phi_x}{\partial x} \right) dx dy \\ k_{14} &= \tilde{e}_{31} \int_V z \left( \frac{\partial u_o^T}{\partial x} \delta \frac{\partial \phi}{\partial z} \right) dv \\ k_{21} &= 0 \\ k_{22} &= k_s G \int_{-b/2}^{b/2} \int_0^L \left( \frac{\partial w_o^T}{\partial x} \delta \frac{\partial w_o}{\partial x} \right) dx dy \\ k_{23} &= -k_s G \int_{-b/2}^{b/2} \int_0^L \left( \delta \frac{\partial w_o^T}{\partial x} \phi_x \right) dx dy \\ k_{24} &= \tilde{e}_{31} \int_V \left( \frac{\partial w_o^T}{\partial x} \delta \frac{\partial \phi}{\partial z} \right) dv \\ k_{31} &= -Ez \int_{-b/2}^{b/2} \int_0^L \left( \frac{\partial \phi_x^T}{\partial x} \delta \frac{\partial u_o}{\partial x} \right) dx dy \\ k_{32} &= -k_s G \int_{-b/2}^{b/2} \int_0^L \left( \phi_x^T \delta \frac{\partial w_o}{\partial x} \right) dx dy \\ k_{33} &= \int_{-b/2}^{b/2} \int_0^L \left( Ez^2 \left( \frac{\partial \phi_x^T}{\partial x} \delta \frac{\partial \phi_x}{\partial x} \right) + k_s G \left( \phi_x^T \delta \phi_x \right) \right) dx dy \\ k_{34} &= -\tilde{e}_{31} \int_V z \left( \frac{\partial \phi_x^T}{\partial x} \delta \frac{\partial \phi}{\partial z} \right) dv \\ k_{41} &= \tilde{e}_{31} \int_V z \left( \frac{\partial \phi^T}{\partial z} \delta \frac{\partial u_o}{\partial x} \right) dv \\ k_{42} &= \tilde{e}_{31} \int_V \left( \frac{\partial w_o}{\partial x} \delta \frac{\partial \phi}{\partial z} \right) dv \end{aligned} \quad (46)$$

$$k_{43} = -\tilde{e}_{31} \int_V z \left( \frac{\partial \phi}{\partial z} \delta \frac{\partial \phi_x}{\partial x} \right) dv$$

$$k_{44} = -\tilde{e}_{zz} \int_V \left[ \left( \frac{\partial \phi}{\partial z} \delta \frac{\partial \phi}{\partial z} \right) \right] dv$$

**Case II: Orthotropic Beam**

The first variations of the strain energy equations number (28)b take the form:

$$\delta U = \int_V \left[ \tilde{Q}_{11} \left[ \left( \frac{\partial u_o}{\partial x} \delta \frac{\partial u_o}{\partial x} \right) - z \left( \frac{\partial u_o}{\partial x} \delta \frac{\partial \phi_x}{\partial x} + \frac{\partial \phi_x}{\partial x} \delta \frac{\partial u_o}{\partial x} \right) + z^2 \left( \frac{\partial \phi_x}{\partial x} \delta \frac{\partial \phi_x}{\partial x} \right) \right] + k_s \tilde{Q}_{55} \left[ \left( \phi_x \delta \phi_x \right) - \left( \phi_x \delta \frac{\partial w_o}{\partial x} + \frac{\partial w_o}{\partial x} \delta \phi_x \right) + \left( \frac{\partial w_o}{\partial x} \delta \frac{\partial w_o}{\partial x} \right) \right] + \tilde{e}_{31} \left[ \left( \frac{\partial u_o}{\partial x} \delta \frac{\partial \phi}{\partial z} + \frac{\partial \phi}{\partial z} \delta \frac{\partial u_o}{\partial x} \right) - z \left( \frac{\partial \phi_x}{\partial x} \delta \frac{\partial \phi}{\partial z} + \frac{\partial \phi}{\partial z} \delta \frac{\partial \phi_x}{\partial x} \right) \right] - \tilde{e}_{ss} \left[ \left( \frac{\partial \phi}{\partial z} \delta \frac{\partial \phi}{\partial z} \right) \right] \right] dv \quad (47)$$

Thus the elements of the stiffness matrix of orthotropic beam can be written as:

$$\begin{aligned} k_{11} &= A_{11} \int_{-b/2}^{b/2} \int_0^L \left( \frac{\partial u_o^T}{\partial x} \delta \frac{\partial u_o}{\delta x} \right) dx dy \\ k_{12} &= 0 \\ k_{13} &= -B_{11} \int_{-b/2}^{b/2} \int_0^L \left( \frac{\partial u_o^T}{\partial x} \delta \frac{\partial \phi_x}{\partial x} \right) dx dy \\ k_{14} &= \tilde{e}_{31} \int_V z \left( \frac{\partial u_o^T}{\partial x} \delta \frac{\partial \phi}{\partial z} \right) dv \\ k_{21} &= 0 \\ k_{22} &= k_s A_{55} \int_{-b/2}^{b/2} \int_0^L \left( \frac{\partial w_o^T}{\partial x} \delta \frac{\partial w_o}{\partial x} \right) dx dy \\ k_{23} &= -k_s A_{55} \int_{-b/2}^{b/2} \int_0^L \left( \delta \frac{\partial w_o^T}{\partial x} \phi_x \right) dx dy \\ k_{24} &= \tilde{e}_{31} \int_V \left( \frac{\partial w_o^T}{\partial x} \delta \frac{\partial \phi}{\partial z} \right) dv \\ k_{31} &= -B_{11} \int_{-b/2}^{b/2} \int_0^L \left( \frac{\partial \phi_x^T}{\partial x} \delta \frac{\partial u_o}{\partial x} \right) dx dy \\ k_{32} &= -k_s A_{55} \int_{-b/2}^{b/2} \int_0^L \left( \phi_x^T \delta \frac{\partial w_o}{\partial x} \right) dx dy \\ k_{33} &= \int_{-b/2}^{b/2} \int_0^L \left( D_{11} \left( \frac{\partial \phi_x^T}{\partial x} \delta \frac{\partial \phi_x}{\partial x} \right) + k_s A_{55} \left( \phi_x^T \delta \phi_x \right) \right) dx dy \end{aligned} \quad (48)$$



$$k_{34} = -\tilde{e}_{31} \int_v \left[ z \left( \frac{\partial \phi_x^T}{\partial x} \delta \frac{\partial \phi}{\partial z} \right) \right] dv$$

$$k_{41} = \tilde{e}_{31} \int_v \left[ z \left( \frac{\partial \phi^T}{\partial z} \delta \frac{\partial u_0}{\partial x} \right) \right] dv$$

$$k_{42} = \tilde{e}_{31} \int_v \left( \frac{\partial w_0}{\partial x} \delta \frac{\partial \phi}{\partial z} \right) dv$$

$$k_{43} = -\tilde{e}_{31} \int_v \left[ z \left( \frac{\partial \phi}{\partial z} \delta \frac{\partial \phi_x}{\partial x} \right) \right] dv$$

$$k_{44} = -\tilde{e}_{zz} \int_v \left[ \left( \frac{\partial \phi}{\partial z} \delta \frac{\partial \phi}{\partial z} \right) \right] dv$$

where;  $A_{ij}$ ,  $B_{ij}$ , and  $D_{ij}$  are the laminate extensional, coupling, and bending stiffness coefficients and they are given by:

$$(A_{11}, B_{11}, D_{11}) = \sum_{n=1}^N \int_{-h/2}^{h/2} \tilde{Q}_{11}(1, z, z^2) dz \quad (49)$$

and

$$A_{55} = \sum_{i=1}^N \int_{-h/2}^{h/2} (\tilde{Q}_{55}) dz$$

By substituting the shape function equations (29), (31), (33) and (39) into Equations (43), (44), (46) and (48), and perform the integration for a beam element with length L, width b and height h, The elements of mass matrix, load vector, and stiffness matrix for both beams are obtained.

### VII. EQUATION OF MOTION

The equation of motion of the whole structure system is represented by [15]:

$$\begin{bmatrix} M_{qq} & 0 \\ 0 & 0 \end{bmatrix} \begin{Bmatrix} \ddot{U} \\ \ddot{\Phi} \end{Bmatrix} + \begin{bmatrix} K_{qq} & K_{q\phi} \\ K_{\phi q} & K_{\phi\phi} \end{bmatrix} \begin{Bmatrix} U \\ \Phi \end{Bmatrix} = \begin{Bmatrix} F \\ G \end{Bmatrix} \quad (50)$$

where  $M_{uu}$  is the global mass matrix of the structure and  $\{U\}$  is generalized displacements coordinates vector,  $\{\Phi\}$  is the generalized electric coordinate's vector describing the applied voltages at the actuators,  $\{F\}$  is the mechanical load vector, and  $\{G\}$  is the electric excitation vector. The proposed finite element model is presented and tested for verification [26] for the analysis of solid Timoshenko beams only. For the present study, a MATLAB code is constructed to perform the static and free vibration analysis of isotropic and orthotropic smart Timoshenko beams with piezoelectric materials. The beams are subjected to different kinds of mechanical and electrical loads. The inputs to the code are the geometric properties of the structure such as the dimensions, the moment of inertia of beam, the adhesive layer, the

piezoelectric layers, number of layers, ply orientations angle, and the material properties of the structure system. The present code is capable of predicting the nodal (axial and transversal) deformation, and the fundamental natural frequency of the beams.

### VII. VALIDATION EXAMPLES

In the following part the behavior of a laminated aluminum beam and a graphite epoxy composite beam with a piezoelectric actuator are investigated using the interactive MATLAB code. The geometry of the smart beam is shown in Figure 3. The different properties of the beams are listed in Table 1 [7].

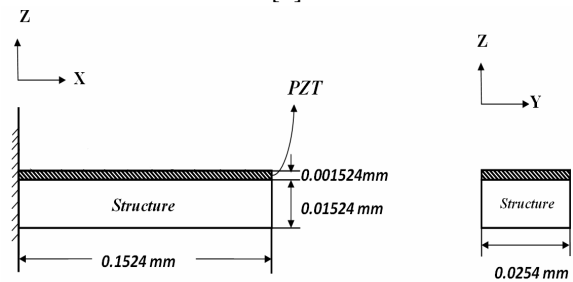


Fig 3: Smart Beam with PZT layer.

Table 1: Material and geometric and material properties of smart beams.

Properties	*Alumin.	*T300/934[0] <sup>0</sup>	*Adhes.	PZT-4
$E_{11}$ (Gpa)	68.9	126	6.9	83
$E_{22}$ (Gpa)	68.9	7.9	6.9	66
$\nu_{12}$	0.25	0.275	0.4	0.31
$G_{12}$ (GPa)	27.6	3.4	2.46	31
$d_{13}$ (m/v)	0	0	0	-122 E-12
$d_{33}$ (m/v)	0	0	0	285 E-12
$\mathcal{E}_{33}^s$ (F/m)	0	0	0	11.53 E-9
$\rho$ (kg/m <sup>3</sup> )	2769	2527	1662	7600
Length (m)	0.1524	0.1524	0.1524	0.1524
Thickness (m)	0.01524	0.01524	0.01524	0.001524
Width (m)	0.0254	0.0254	0.0254	0.0254

\* Reference 7.

### VIII. CONVERGENCE OF THE PROPOSED MODEL RESULTS

Figure 4 and Figure 5 show the convergence of the transverse deflection with the number of elements for both isotropic and orthotropic smart beams. The obtained results prove the convergence of the predicted results of the present finite element model.

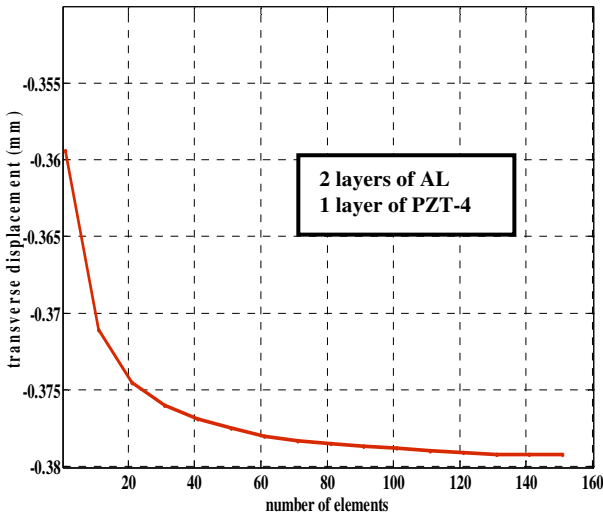


Fig 4: Transverse deflection vs. number of elements for smart isotropic beam

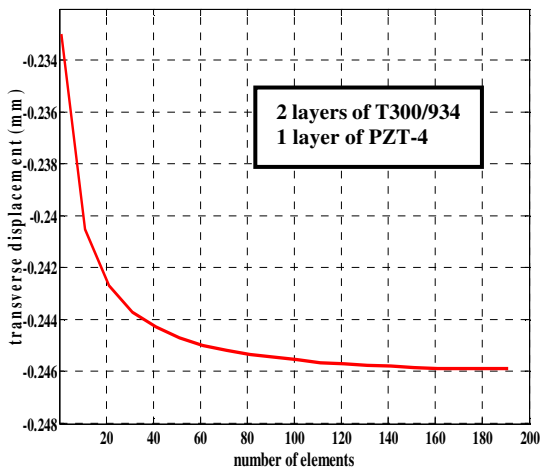


Fig 5: Transverse deflection vs. number of elements for smart orthotropic beam

IX. SMART BEAMS RESULTS

A. Static analysis

Each of isotropic aluminum or orthotropic T300/934 composite Graphite/epoxy [0], PZT smart beams with its respective data listed in Table 1 is subjected to a constant electric potential of 12.5 kV. The electric load was applied on the upper surface of the PZT-4 layer, while the lower surface was grounded (0 V) [15]. A number of elements of twenty are used, the parameter ( $e_{31} = c_{11}d_{31}$ ), and shear correction factor  $k_s$  of 5/6 are taken. Figure 6 and Figure 7 show the predicted transverse deflections for both isotropic and orthotropic beams. Good agreement is generally obtained between the obtained results of the present model and that obtained by Refs. [11]-[7]-[15].

The Effect of number of layers of the beams on the transverse deflection is shown in Figure (8) and they compare with the results obtained by Ref. [15]. It is seen

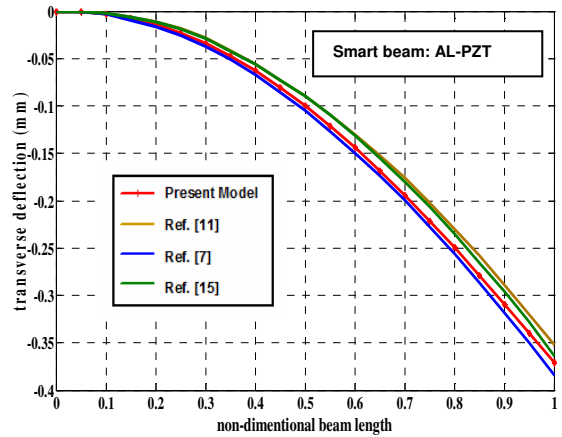


Fig 6: Transverse deflections for Aluminum beam with PZT

from the figure that as the number of layers increases, the beam stiffness increases, and the non-dimensional transverse deflection decreases. Figures (9) and (10) present the effect of the applied voltages on the transverse displacements of aluminum beam and T300/934 Graphite/epoxy [0] composite beam with PZT-4 actuator, respectively. It is seen from both figures that the transverse displacement increases with the increase of applied voltage.

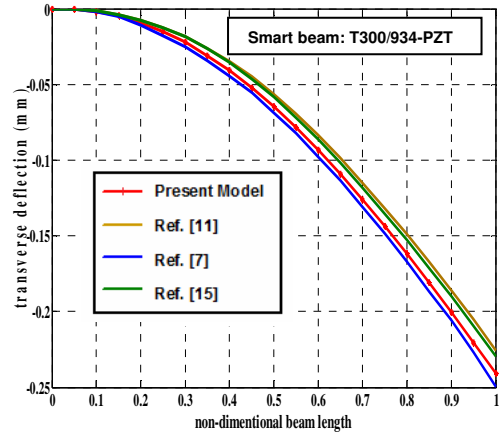


Fig 7: Transverse deflections for T300/934 composite beam with PZT.

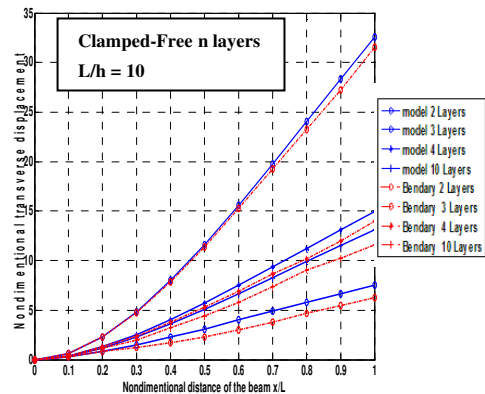


Fig 8: Non-dimensional transverse deflection vs. non-dimensional distance along the beam length.

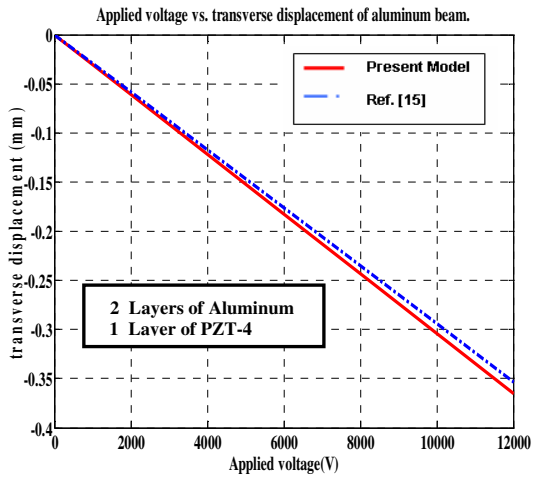


Fig 9: Transverse displacement vs. applied voltage for aluminum beam with piezoelectric actuator.

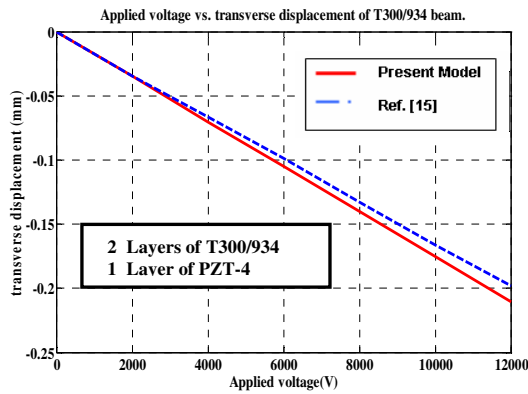


Fig 10: Transverse displacement vs. applied voltage for T300/934 composite beam with piezoelectric actuator.

Figures (11) and (12) show the effect of applied voltage on the axial displacements of the same beams. It is seen from both figures that the axial displacement increases almost linearly with increasing the applied voltages. In addition, the increased value of axial displacement is found to be an order of magnitude smaller than the increased value of the transverse displacement.

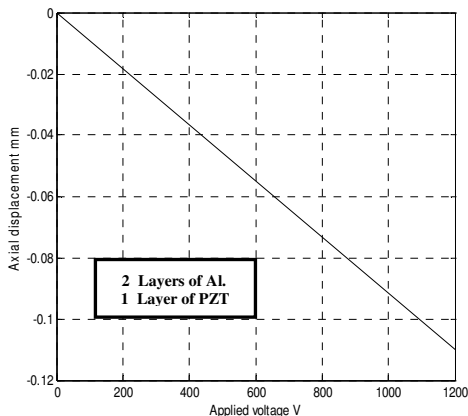


Fig 11: Axial displacement vs. applied voltage for aluminum beam with piezoelectric actuator.

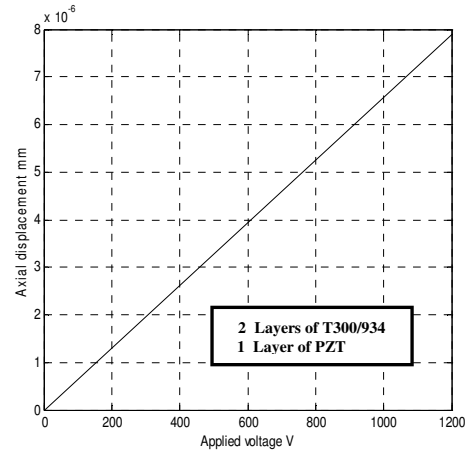


Fig 12: Axial displacement vs. applied voltage for T300/934 composite beam with piezoelectric actuator.

**B. Dynamic Analysis**

Table 2 shows the predictions of the fundamental natural frequencies of the aluminum beam compared with other references [7]-[8]-[15] when the applied voltage on the upper surface of the PZT-4 is equal to zero. Excellent agreement is obtained by the present model using number of elements of twenty.

Table 2: Predicted natural frequencies of aluminum beam with single PZT- 4 layer.

No of elements	Natural frequencies			
	Ref. [7]	Ref. [8]	Ref. [15]	Present Model
10	539.3	539.7	530.9	540.5
20	538.6	539.3	530.9	539.3
30	538.5	539.1	530.8	539.1

The obtained results of the proposed finite element model based on Timoshenko beam theory prove its validity and predictive capabilities in comparison with the results of some models proposed by other investigators as follows:

1. The model does not need more computational effort as the layer wise method proposed by [7] which has great number of degrees of freedom used. In addition, the present model has the following advantages:
2. It is suitable for predicting the response of moderate laminate thicknesses and smart structure system which entails additional heterogeneity from the piezoelectric layer and induced strain actuation [7]-[9].
3. The present model has better predictions compared to the model proposed by [15] which used the CBT theory for modeling without taking the shear effect into consideration.

4. The use of the shear correction factor improved the present model prediction.
5. The predictions of the present model have lower accuracy than the predictions of the model proposed by [11] because the mathematical model of Ref. [11] was based on a high order displacement field coupled with a layer wise linear electric potential. However, the predictions of the present model with suitable number of elements not only gives close results to that predicted by the model of Ref. [11], but also it does not need a computational effort as this reference done.
6. The present model allows any element to be non-active or active (an actuator or a sensor).

### X. CONCLUSION

A finite element model has been proposed to predict the static and the free vibration characteristics of laminated aluminum and fiber reinforced composite beams with piezoelectric materials using Timoshenko beam theory. The following points have been drawn:

1. A good agreement between the present model predictions using Timoshenko beam theory, and the corresponding predicted results of other investigators using, classical beam theory, layer wise theory, and HODT. This proves the predictive capabilities of such model with less computational effort.
2. The present model predictions was better than the results obtained by a simple Euler-Bernoulli's beam theory, CBT but it required more computational effort due to inclusion of the transverse shear effects.
3. The validity for representing the electric potential as a function of the length and the thickness of the beam in the proposed model.
4. The proposed model prediction were obtained at reasonable number of elements.
5. As the applied voltage increases both the transverse and axial displacements increase, respectively.
6. As the number of layers increases, the transverse deflection decreases with the applied voltage.
7. The inclusion of shear correction factor improved the model predictions.
8. The model can be extended to the following future work:
  - a) Using the simple higher order shear deformation theory made by Reedy, to improve the predictions of the transverse shear effects.
  - b) Taking into account the geometric nonlinearities in the finite element model which may improve the obtained results.

### REFERENCES

- [1] A. A. Khdeir and J.N. Reddy, "An Exact Solution for the Bending of Thin and Thick Cross-Ply Laminated Beams", Computers & Structures, Vol. 37, pp.195-203, 1997.
- [2] K. Chandrashekhara and K.M. Bangera, "Free Vibration of Composite Beams Using a Refined Shear Flexible Beam Element", Computers and Structures, Vol. 43, No.4, pp.719-727, 1992.
- [3] S.M. Nabi and N. Ganesan, "Generalized Element for the Free Vibration Analysis of Composite Beams", Computers & Structures, Vol. 51, No. 5, pp. 607-610,1994.
- [4] V. Yildirm, E. Sancaktar and E. Kiral, "Comparison of the In-Plan Natural Frequencies of Symmetric Cross-Ply Laminated Beams Based On The Bernoulli-Eurler and Timoshenko Beam Theories", J. of Appl. Mech., Vol. 66, pp. 410-417, 1999.
- [5] A. Henno and T.J.R. Huges, "Finite Element Method for Piezoelectric Vibration", Int. J. for Numerical Methods in Engineering", Vol. 2, pp. 151-157,1970.
- [6] E.F. Crawley and K.B. Lazarus, "Induced Strain Actuation of Isotropic and Anisotropic Plates", AIAA J., Vol. 29, No. 6, pp. 944-951, 1991.
- [7] D.A. Saravanos and P.R. Heyliger, "Coupled Layer wise Analysis of Composite Beams with Embedded Piezoelectric Sensors and Actuators", J. of Intelligent Material Systems and Structures, Vol. 6, pp. 350-363, 1995.
- [8] D.H. Robbins and J.N. Reddy, "Analysis of Piezoelectric ally Actuated Beams Using A Layer-Wise Displacement Theory", Computers & Structures, Vol. 41, No.2, pp. 265-279, 1991.
- [9] Q. Wang and S.T. Quek, "Dispersion Relations In Piezoelectric Coupled Beams", AIAA J., Vol. 38, No. 12, pp. 2357-2361,1996.
- [10] A. Benjeddou, M.A. Trindade and R. Ohayon, "A Unified Beam Finite Element Model for Extension and Shear Piezoelectric Actuation Mechanisms", J. Intelligent material systems and structures, Vol. 8, No. 12, pp. 1012-1025, 1997.
- [11] Y.K. Clinton Chee, L. Tong and P.S. Grant, "A mixed Model for Composite Beams with Piezoelectric Actuators and Sensors", Smart Materials and Structures, Vol. 8, pp. 417-432, 1999.
- [12] K.K. Ang, J.N. Reddy and C.M. Wang, "Displacement Control of Timoshenko Beams via Induced Strain Actuators", Smart Materials and Structures, Vol.9, pp.981-984, 2000.
- [13] ZHOU Yan-guo; CHEN Yun-min; and DING Hao-jiang, "Analytical Modeling and Free Vibration Analysis of Piezoelectric Bimorphs", Journal of Zhejiang University Science, 6A (9): 938-944, 2005.

- [14] C.W.H. Lau, C.W. Lim and A.Y.T. Leung, "A Variational Energy Approach for Electromechanical Analysis of Thick Piezoelectric Beam", Journal of Zhejiang University Science, 6A (9): pp. 962-966, 2005.
- [15] M. Adnan Elshafei<sup>1</sup>, I M Bendary and A M Riad "Finite Element Model of Smart Beam with Distributed Piezoelectric Actuators", J. of Intelligent Material Systems and Structures, 21: 747-758, 2010.
- [16] T. M. Seigler, A. H. Ghasemi, and A. Salehian, "Distributed Actuation Requirements of Piezoelectric Structures under Servo constraints", J. of Intelligent Material Systems and Structures, Vol. 22: 1227, 2011.
- [17] P.Vidal, M. D'Ottavio, M. Ben Thai..er, and Polit Olivier, "An Efficient Finite Shell Element for the Static Response of Piezoelectric Laminates", J. of Intelligent Material Systems and Structures, Vol. 22: 671, 2011.
- [18] F. Biscani, P. Nali, S. Belouettar, and E. Carrera, 'Coupling of hierarchical piezoelectric plate finite elements via Arlequin method', J. of Intelligent Material Systems and Structures, Vol. 23: 749, 2012.
- [19] F. Cottone, L. Gammaitoni, H. Vocca, M. Ferrari, and V. Ferrari, "Piezoelectric buckled beams for random vibration Energy Harvesting", Smart material and Structure, Vol. 21, pp1-11, 2012.
- [20] J.N. Reddy<sup>1</sup>, "An Introduction to Nonlinear Finite Element Analysis ", Oxford University Press, USA, 2004.
- [21] W. G. Cady, "Piezoelectricity", Dover NY and McGraw Hill Publications, NY, USA, 1964.
- [22] "IEEE Standard on Piezoelectricity"; ' IEEE Std. 176-1978', The Institute of electrical and electronics engineers, Inc., NY, USA, pp. 12, 1978.
- [23] T. Ikeda, "Fundamental of Piezoelectricity", Oxford Univ. Press Inc., Printed in the USA, pp. 5-17, 1996.
- [24] M. Adnan Elshafei<sup>2</sup>, "Smart Composite Plate Shape Control Using Piezoelectric Materials"; Ph.D. Dissertation, US Naval Postgraduate School, pp57-61, Sep.1996.
- [25] J. N. Reddy<sup>2</sup>, "Mechanics of Laminated Composite Plates and Shells, Theory and Analysis", 2nd Edition, CRC Press, USA, p102, 2004.
- [26] M Adnan Elshafei<sup>3</sup>, "FE Modeling and Analysis of Isotropic and Orthotropic Beams Using First Order Shear Deformation Theory", J. Materials Sciences and Applications, 4:77-102, 2013.